Frontiers in Heat and Mass Transfer

Available at www.ThermalFluidsCentral.org

NUMERICAL STUDY OF STAGNATION POINT FLOW OF CASSON FLUID OVER A CONTINUOUS MOVING SURFACE

Muhammad Amin Murad[a,*] Faraidun Hamasalh[b], Hajar F. Ismael[c]

[a] Department of Mathematics, College of Science, University of Duhok, Duhok, 42001, Iraq
[b] Department of Mathematics, College of Education, University of Sulaimani, Sulaimani, 46001, Iraq
[c] Department of Mathematics, Faculty of Science, University of Zakho, Zakho, 42002, Iraq

ABSTRACT

In this paper, we study the behavior of heat transfer of Casson fluid at the magnetohydrodynamic stagnation point with thermal radiation over a continuous moving sheet. The appropriate similarity transfer is used to transfer the governing differential equations into the ordinary differential equation and then solved by the collocation method based on spline function. The obtained results are investigated with the existing literature by direct comparison. We found that an increment in the value of the shrinking parameter, magnetic parameter, and Casson fluid parameter enhances the velocity distribution and depreciate the temperature profile both Casson and Newtonian fluids. Furthermore, the thermal distribution depreciates with increasing the value of Prandtl number and radiation parameter for Casson and Newtonian fluids. Finally, the impact of the emerged physical parameters on the velocity and temperature distributions are illustrated via tables and illustrative graphs.

Keywords: *Casson fluid, magnetohydrodynamic, collocation spline method, magnetic field.*

1. INTRODUCTION

Convection boundary layer flow on a continuous moving sheet is utilized in different industrial processes, including the manufacturing electrolyte paper, thinning and annealing of conductive material, and the drawing thermoplastic. The boundary layer flow over a shrinking\stretching surface is widely used in different industrial processes, including the manufacturing electrolyte paper, thinning and annealing of conductive material, and polymer processing. Hiemenz (1911) was the first to investigate the conventional two-dimensional unsteady flow on a flat sheet. Sakiadis (1961) initiated an investigation on the flow through a continuous moving surface. The concept of a stretching surface of boundary layer flow of viscous fluid initiated via Crane (1970). Following that, many scholars continued to detect the flow over a continuous moving surface from different perspectives (Gupta and Gupta, 1977; Ganesh and Sridhar, 2021; Al-Sawalmeh, 2022; Murad and Hamasalh, 2022). However, the non-Newtonian flow is found in a variety of large-scale industrial process such as blood flow models, polymer, thinning and annealing of conductive material, and ice flows. Several fluids are considered as non-Newtonian fluid like Williamson fluid, and power law fluid flow. A shear-thinning Casson fluid that generates the yield of shear stresses is also a non-Newtonian fluid. Due to its rheological properties, the Casson fluid has been classified as the most popular non-Newtonian fluid. The yield shear stress behaves like a solid when it is greater than the shear stress while the liquid starts to move when the yield shear stress is less than the shear stress, such as human blood, fruit juice, and tomato sauce. The Casson fluid has major applications in different aspects of real life like in cancer homeo-therapy and fibrinogen. Due to these significant advantages, it has been an area of interest to many researchers. The Casson fluid was first introduced by

Casson (1959). The analysis of Casson fluid over various geometries are presented in (Malik et al., 2014; Babu et al., 2017; El-Aziz and Afify, 2016; Rani et al., 2021). Magnetohydrodynamic is the physical characteristic that explains the behavior of a highly conducting fluid in the presence of a magnetic field. The conductive fluids produce an electrical current due to the liquid flow, and generated force increases the mechanical behaviors of the liquid. The electrically conducting peristaltic flow has considerable implementation in the biological fluids: such as blood flows, peristalsis flows, and nano fluid see (Mekheimer, 2008; Hayat et al., 2010; Sandeep et al., 2013). Over a continuously stretched sheet the effects of magnetic field and thermal transfer on the Casson fluid boundary layer flow is studied by Dhange et al. (2022). In the existence of mass transfer and heat transfer, the Casson fluid flow of an optically thick fluid along a vertically inclined surface analyzed by Raju et al. (2017). A three-dimensional Casson fluid through a thin linearly stretched plate with convection constrain is studied in Mahanta and Shaw (2015). 3D MHD stagnation point flow of an incompressible Casson fluid in the porous material is studied by Shahzad et al. (2015). 3D Casson-Carreau fluid in an unsteady stretched sheet is investigated by Raju and Sandeep (2016). The Casson fluid flow over a vertical porous sheet electronically conducting considering the impact of the generated magnetic field is studied by Goswami and Sarma (2021). The dual solutions for a Casson fluid's thermal properties and heat transfer enhancement over a porous continuous moving surface are analyzed in Khan et al. (2021). Aziz and Afify (2019) studied the magnetohydrodynamic Casson fluid flow across stretching surface with viscous dissipation estimation and Hall effects.

This paper aims to extend the analysis of MHD stagnation points flow of Casson fluid over a continuous moving surface electrically conducting in the presence of thermal radiation and transverse magnetic field with the effect of Caputo derivative. The Maple 2020 program is employed to

---

* *Corresponding author. Email: muhammad.math@uod.ac*

solve the converted mathematical problem using the collocation method based on spline function (CMSF) and the Runge Kutta method (rkf45). Numerical and graphical representations of the effect of emerging physical parameters on velocity and thermal distribution are provided.
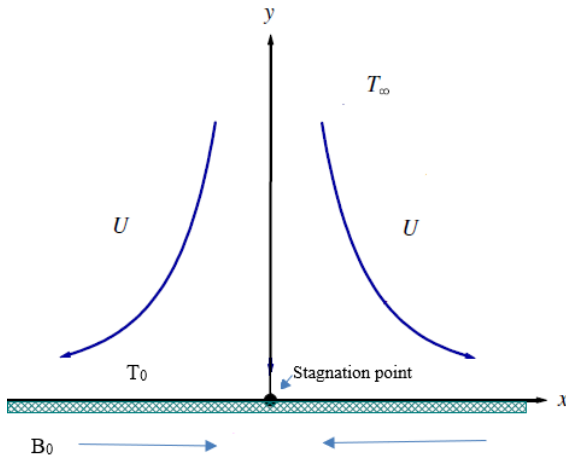
Fig. 1 The skitch of the present model.

2. MATHEMATICAL MODEL

The Consider 2D magnetohydrodynamic stagnation point flow of an incompressible viscous Casson fluid flow electrically conducting impinging normally over a heated continuous moving surface. Assume that the magnetic Renolds number is represented by small Shercliff (1965) and the velocity field U and the uniform stationary magnetic field of strength B_0 are perpendicular. Here, the produced magnetic field is disregarded as compared to the imposed field. The electric field is zero, no polarization voltage is supplied. In addition, the boundary layer and Boussinesq approximations are assumed to be valid. The equations of motion of steady 2D magnetohydrodynamic incompressible viscous boundary layer Casson fluid flow are given as follows

$$\frac{\partial u}{\partial x} + \frac{\partial v}{\partial y} = 0, \tag{1}$$

$$u\frac{\partial u}{\partial x} + v\frac{\partial u}{\partial y} = \frac{\lambda}{\rho}\frac{\partial^2 u}{\partial y^2} - \frac{1}{\rho}\frac{\partial p}{\partial x} + v\left(1+\frac{1}{\beta}\right)\frac{\partial^2 u}{\partial y^2} + \frac{\sigma_e B_0^2}{\rho}(U-u). \tag{2}$$

The electric conductivity of the fluid is σ_e, the pressure represented by p and U represents the free stream velocity of the fluid. In the absence of the viscous dissipation the thermal allocation equation for our boundary value problem is as follows:

$$\rho c\left(u\frac{\partial T}{\partial x} + v\frac{\partial T}{\partial y}\right) = \kappa_0\frac{\partial^2 T}{\partial x^2} - \frac{\partial q}{\partial y}, \tag{3}$$

when c is the given thermal ability at fixed pressure of the fluid, T is the temperature, κ_0 represents the heat conductivity constant, and q is the radiative heat flux. The radiative thermal flow using Resseland approximation Raptis et al. (2004) is simplified as follows

$$q = \frac{4\sigma}{3k}\left(\frac{\partial T}{\partial y}\right)^4, \tag{4}$$

when σ represents the mean absorption coefficient and k represents the Stefan-Boltzmann number. T^4 is the temperature fluctuation inside the

flow which is considered as a linear function of temperature. Appling the Taylor series about T^∞ for expanding T^4.

$$T^4 \simeq 4T_\infty^3 T - 3T_\infty^4. \tag{5}$$

Taking Eqs. (4) and (5), The Eq. (3) is reduced to

$$u\frac{\partial T}{\partial x} + v\frac{\partial T}{\partial y} = \frac{1}{\rho c}\left(k_0 + \frac{16\sigma T_\infty^3}{3k}\right)\frac{\partial^2 T}{\partial y^2}. \tag{6}$$

The above equation depicts that the enhance of thermal conductivity is due to the impact of radiation. Assume that $Nr = \dfrac{kk_0}{4\sigma T_\infty^3}$ is the radiation parameter. Thus, Eq. (6) becomes

$$u\frac{\partial T}{\partial x} + v\frac{\partial T}{\partial y} = \frac{k_0}{k}\frac{\partial^2 T}{\partial y^2} \tag{7}$$

where $k = \dfrac{Nr}{Nr+\dfrac{4}{3}}$.

Consider the following boundary conditions of the present problem

$$u(x,y) = bx, v(x,y) = 0, T(x,y) = T_0, y \to 0$$
$$u(x,y) = U = ax,, \qquad T(x,y) = T_\infty, y \to \infty. \tag{8}$$

Here, $b > 0$ represents the shrinking ratio, T_0 represents the thermal sheet and the temperature of the liquid outside represented by T_∞. Now, solving governing Eq. (1), Eq. (2) and Eq. (6) with the given boundary conditions (8) gives the velocity and temperature fields for the proposed model. Hence, the following similarity transform is given

$$\eta = \left(\frac{a}{v}\right)^{0.5} y, p(x,\infty) = p_0 - \frac{1}{2}(x^2+y^2)a^2\rho,$$

$$u(x,y) = xaf'(\eta), v(x,y) = -f(\eta)(av)^{0.5}, \tag{9}$$

$$\theta(\eta) = (T - T_\infty)(T_0 - T_\infty)^{-1},$$

when η represents the similarity parameter, p_0 and a are the strength of stagnation point and the stagnation pressure respectively. Satisfying the Eq. (9) in Eq. (1) and Eq. (2), the continuity Eq. (1) is satisfied and the possible fluid motion is represented by velocity field, and then putting Eq. (9) in Eq. (3) with some simple calculations, we obtain

$$\left(1+\frac{1}{\beta}\right)f''' + ff'' - f'^2 + M^2(1-f') + 1 = 0. \tag{10}$$

Putting Eq. (9) in Eq. (7), we obtain

$$\frac{1}{\text{Pr}}\theta'' + k\theta'f = 0. \tag{11}$$

Now, $M = \left(\dfrac{B_0^2\sigma_e}{a\rho}\right)^{0.5}$ is magnetic field parameter or (Hartmann number) and $\text{Pr} = c\mu\kappa_0^{-1}$ Prandtl number. Also, $k = 3Nr(3Nr+4)^{-1}$ where Nr is radiation parameter.

The considered boundary conditions in Eq. (8) with taking the dimensionless parameters in consideration, we obtain the following boundary conditions:

$$f(0) = 0, f'(0) = B = \frac{b}{a}, \ f'(\infty) = 1, \tag{12}$$

$$\theta(0) = 1, \theta(\infty) = 0.$$

where a and b are real constant, and B is shrinking parameter.

3. COLLOCATION SPLINE METHOD

In this section, the spline interpolations (De Boor and De Boor, 1978; Schumaker, 2015) are proposed to solve the boundary value problems presented in Eq. (9) and Eq. (10) to gather with the boundary conditions (11). First, we present the cubic spline approach which is used by Bickley over two-point boundary value problem Bickley (1968), and then used by Izyan et al. (2017) to investigate free motion of layered truncated conical shells filled with quiescent fluid. The Bickley cubic spline is given by

$$S(\eta) = a_0 + a_1(\eta - \eta_0) + \frac{1}{2}a_2(\eta - \eta_0)^2 + \frac{1}{6}\sum_{i=0}^{n-1} d_i(\eta_n - \eta_i)_+^3. \quad (13)$$

To solve third order boundary value problem, we need to have a spline approach of higher degree. Hence, consider the following quartic spline

$$S(\eta) = a_0 + a_1(\eta - \eta_0) + \frac{1}{2}a_2(\eta - \eta_0)^2 + \frac{1}{6}d_0(\eta - \eta_0)^3 + \frac{1}{24}\sum_{i=0}^{n-1} b_i(\eta_n - \eta_i)_+^4. \quad (14)$$

Here, we define the power function $(\eta - \eta_i)_+$ as follows:

$$(\eta - \eta_i)_+ = \begin{cases} \eta - \eta_i & \eta_i < \eta \\ 0 & otherwise. \end{cases}$$

Consider the equally spaced knots of partition $\Omega : \tilde{a} = \eta_0 < \eta_1 < ... < \eta_n = \tilde{b}$ on $[\tilde{a}, \tilde{b}]$. Assume that $S_4(\Omega)$ is the space of quartic polynomials on Ω which is continuously differentiable piecewise.

Consider the following third order boundary value problem of fractional order:

$$f^{(\alpha)}(\eta) + p(\eta)f''(\eta) + q(\eta)f'(\eta) + r(\eta)f(\eta) = m(\eta), \ \tilde{a} \le \eta \le \tilde{b}, \ 2 < \alpha \le 3, \quad (15)$$

associated with the following boundary conditions:

$$\alpha_0 f_0 + \beta_0 f_n' + \gamma_0 f_n'' = \lambda_0,$$
$$\alpha_1 f_0' + \beta_1 f_n + \gamma_1 f_n'' = \lambda_1, \quad (16)$$
$$\alpha_2 f_0'' + \beta_2 f_n + \gamma_2 f_n' = \lambda_2,$$

where $f^{(\alpha)}(\eta)$ represents the Caputo derivative (Malo et al., 2021; Murad, 2022) of $f(\eta)$ and the functions $f(\eta), p(\eta), q(\eta), r(\eta), m(\eta)$ are continuous functions in $[\tilde{a}, \tilde{b}]$.

Now, we substitute $S(\eta), S'(\eta), S''(\eta), S^{(\alpha)}(\eta)$ of quartic spline (13) into the boundary value problem (15), we obtain

$$\sum_{i=0}^{n-1} b_i \left\{ \frac{\Gamma(5)}{\Gamma(5-\alpha)}(\eta_j - \eta_i)_+^{4-\alpha} + \frac{1}{2}p_j(\eta_j - \eta_i)_+^2 + \frac{1}{6}q_j(\eta_j - \eta_i)_+^3 + \frac{1}{24}r_j(\eta_j - \eta_i)_+^4 \right\}$$

$$+a_3 \left\{ \frac{1}{6}\frac{\Gamma(4)}{\Gamma(4-\alpha)}(\eta_j - \eta_0)^{3-\alpha} + p_j(\eta_j - \eta_0) + \frac{1}{2}q_j(\eta_j - \eta_0)^2 + \frac{1}{6}r_j(\eta_j - \eta_0)^3 \right\}$$

$$+a_2 \left\{ p_j + q_j(\eta_j - \eta_0) + \frac{1}{2}r_j(\eta_j - \eta_0)^2 \right\}$$

$$+a_1 \left\{ p_j + r_j(\eta_j - \eta_0) \right\} + a_0 \left\{ r_j \right\} = m\{\eta_j\}, \ j = 0,1,2,...,n.$$

From boundary conditions (16), we obtain

$$\sum_{i=0}^{n-1} b_i \left(\frac{\beta_0}{6}(\tilde{b} - \eta_i)_+^3 + \frac{\gamma_0}{2}(\tilde{b} - \eta_i)_+^2 \right) + a_3 \left(\frac{\beta_0}{2}(\tilde{b} - \tilde{a})^2 + \gamma_0(\tilde{b} - \tilde{a}) \right)$$

$$+a_2 \left(\beta_0(\tilde{b} - \tilde{a}) + \gamma_0 \right) + a_1\beta_0 + a_0\alpha_0 = \lambda_0,$$

$$\sum_{i=0}^{n-1} b_i \left(\frac{\beta_1}{24}(\tilde{b} - \eta_i)_+^4 + \frac{\gamma_1}{2}(\tilde{b} - \eta_i)_+^2 \right) + a_3 \left(\frac{\beta_1}{6}(\tilde{b} - \tilde{a})^3 + \gamma_1(\tilde{b} - \tilde{a}) \right)$$

$$+a_2 \left(\frac{\beta_1}{2}(\tilde{b} - \tilde{a})^2 + \gamma_1 \right) + a_1 \left(\beta_0(\tilde{b} - \tilde{a}) + \alpha_1 \right) + a_0\beta_1 = \lambda_1,$$

$$\sum_{i=0}^{n-1} b_i \left(\frac{\beta_2}{24}(\tilde{b} - \eta_i)_+^4 + \frac{\gamma_2}{6}(\tilde{b} - \eta_i)_+^3 \right) + a_3 \left(\frac{\beta_2}{6}(\tilde{b} - \tilde{a})^3 + \frac{\gamma_2}{2}(\tilde{b} - \tilde{a})^2 \right)$$

$$+a_2 \left(\frac{\beta_2}{2}(\tilde{b} - \tilde{a})^2 + \gamma_2(\tilde{b} - \tilde{a}) + \alpha_2 \right) + a_1 \left(\beta_2(\tilde{b} - \tilde{a}) + \gamma_2 \right) + a_0\beta_2 = \lambda_2.$$
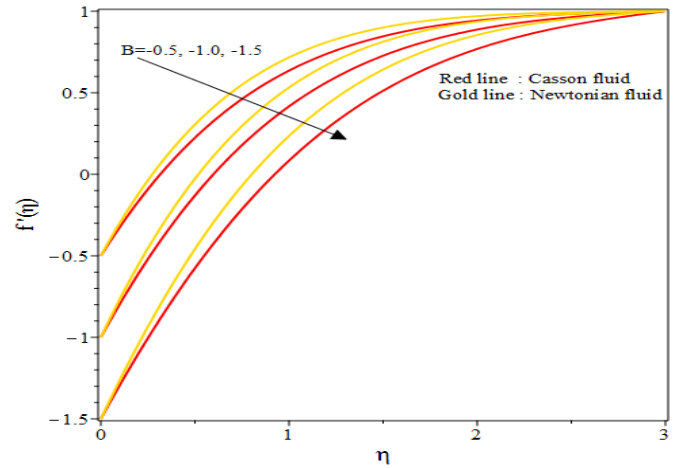
Fig. 2 The impact of shrinking parameter B on the velocity profile $f'(\eta)$.
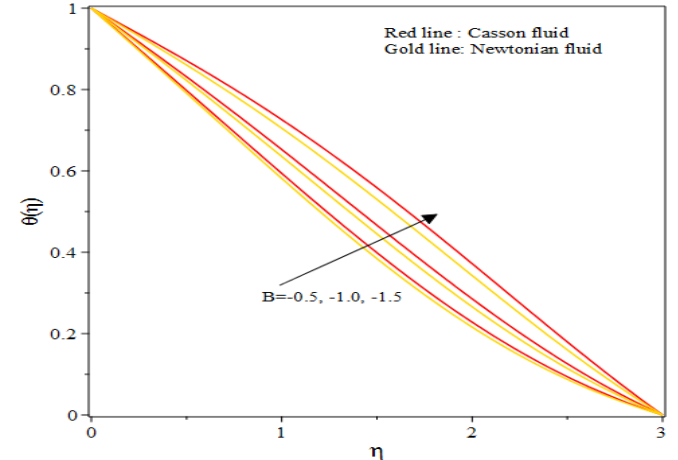
Fig. 3 The impact of shrinking parameter B on the temperature profile $\theta(\eta)$.

4. QUASI LINEARIZATION TECHNIQUE (QLT)

To approximate a non-linear Ordinary differential equation to a linear Ordinary differential equation the QLT algorithm is used. The technique depends on Newton-Raphson technique which was found by Mandelzweig and Tabakin (2001). The QLT is widely utilized in different fields of science like applied mathematics and astronomy Parand et al. (2009). The approximate linear ODE driven by QLT cannot be solved analytically, thus the collocation method based on B-spline function is presented to solve the proposed problem numerically. Here, we apply the QLT to the present problem the approximate linear differential equation at the $(m+1)$ iteration given by:

$$\frac{d^3 f}{d\eta^3} = \Omega(f''(\eta), f'(\eta), f(\eta), \eta), \quad (17)$$

$$\frac{d^2 \theta}{d\eta^2} = \Theta(\theta'(\eta), \theta(\eta), \eta), \quad (18)$$

3
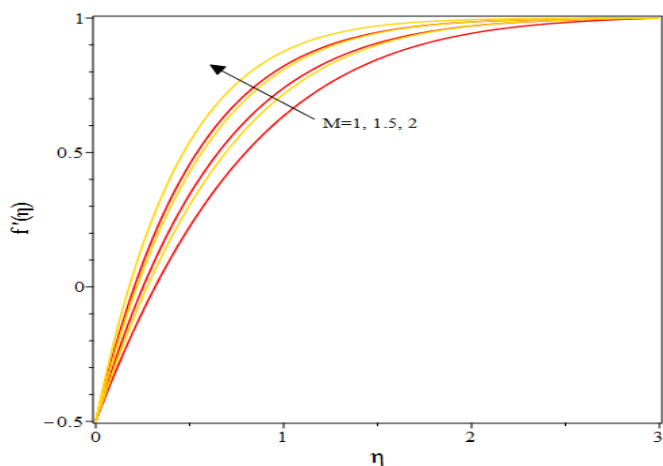
Fig. 4 The impact of magnetic field parameter M on the velocity profile $f'(\eta)$.
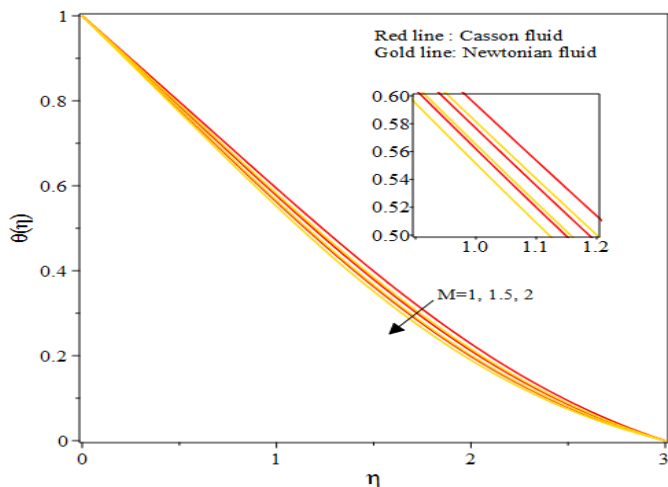
Fig. 5 The impact of magnetic field parameter M on the temperature profile $\theta(\eta)$.

Using Eq. (9), we obtain

$$\Omega\left(f''(\eta),f'(\eta),f(\eta),\eta\right)=\left(\frac{\beta}{\beta+1}\right)\left(f'(\eta)^2-f(\eta)f''(\eta)-M^2\left(1-f'(\eta)\right)-1\right),\quad(19)$$

$$\Theta\left(\theta'(\eta),\theta(\eta),\eta\right)=-\Pr k\,\theta'(\eta)f(\eta).\qquad(20)$$

To solve Eq. (10) and Eq. (11) employing spline collocation approach, it requires to transfer nonlinear problem into linear form. Thus, by using quasi-linearization technique Eq. (10) and Eq. (11) convert to the following linear forms. The QLT formula is defined as follows:

$$\frac{d^3 f_{m+1}}{d\eta^3}=\Omega(f_m'',f_m',f_m,\eta)-(f_m-f_{m+1})\Omega_f(f_m'',f_m',f_m,\eta)$$
$$-(f_m'-f_{m+1}')\Omega_{f'}(f_m'',f_m',f_m,\eta)-(f_m''-f_{m+1}'')\Omega_{f'}(f_m'',f_m',f_m,\eta),\qquad(21)$$

$$\frac{d^2\theta}{d\eta^2}=\Theta(\theta_m',\theta_m,\eta)-(\theta_m-\theta_{m+1})\Theta_\theta(\theta_m',\theta_m,\eta)-(\theta_m'-\theta_{m+1}')\Theta_{\theta'}(\theta_m',\theta_m,\eta).\qquad(22)$$

Now, applying QLT on Eq. (10) and Eq. (11), we obtain

$$\left(\frac{1}{1+\beta}\right)f_{m+1}'''+f_m f_{m+1}''+f_{m+1}f_m''-2f_m'f_{m+1}'-M^2 f_{m+1}'=f_m f_m''-f_m'^2-\left(M^2+1\right),\qquad(23)$$

$$\theta_{m+1}''(\eta)-\Pr k\,\theta_{m+1}'(\eta)f_m(\eta)=0.\qquad(24)$$

Here, we can convert Eq. (23) to a third order differential equation of fractional order as follows

$$\left(\frac{1}{1+\beta}\right)f_{m+1}^{(\alpha)}+f_m f_{m+1}''+f_{m+1}f_m''-\left(2f_m'+M^2\right)f_{m+1}'=f_m f_m''-f_m'^2-\left(M^2+1\right),\qquad(25)$$

$$2<\alpha\le 3$$

$$\theta_{m+1}''(\eta)-\Pr k\,\theta_{m+1}'(\eta)f_m(\eta)=0.\qquad(26)$$

with the following boundary conditions:

$$f_{m+1}(0)=0,f_{m+1}'(0)=B,f_{m+1}'(\infty)=1,$$
$$\theta_{m+1}(0)=1,\theta_{m+1}(\infty)=0,\qquad(27)$$

where $f^{(\alpha)}(\eta)$ represents the Caputo derivative of $f(\eta)$. The system of the collocation equations using Eq. (26) and Eq. (27) for f have the following form

$$\sum_{i=0}^{n-1}b_i\left[\frac{\Gamma(5)}{24\Gamma(5-\alpha)}(\eta_m-\eta_i)^{4-\alpha}+\frac{f_m}{2}(\eta_m-\eta_i)^2-\frac{1}{6}(2f_m'+M^2)(\eta_m-\eta_i)^3+\frac{f_m''}{24}(\eta_m-\eta_i)^4\right]$$

$$+d_0\left[\frac{\Gamma(4)}{6\Gamma(4-\alpha)}(\eta-\eta_0)^{3-\alpha}+f_m(\eta-\eta_0)-\frac{1}{2}(2f_m'+M^2)(\eta-\eta_0)^2+\frac{1}{6}f_m''(\eta-\eta_0)^3\right]$$

$$+a_2\left[f_m-\frac{1}{2}(2f_m'+M^2)(\eta-\eta_0)+\frac{f_m''}{2}(\eta-\eta_0)^2\right]$$

$$+a_1\left[-f_m''(\eta-\eta_0)+(2f_m'+M^2)\right]+a_0\left[f_m''\right]=f_m f_m''-f_m'^2-(M^2+1),m=0,1,2,...,n\qquad(28)$$

and the system of collocation equations for the temperature θ has the following form

$$\sum_{i=0}^{n-1}d_i\left[(\eta_m-\eta_i)+\frac{\Pr k f_m}{2}(\eta_m-\eta_i)^2\right]+a_2\left[1+\Pr k f_m(\eta_m-\eta_i)\right]+a_1\left[\Pr k f_m\right]\qquad(29)$$

and the boundary conditions (27) becomes

$$a_0+a_1(\tilde{a})+\frac{1}{2}a_2(\tilde{a})^2+\frac{1}{6}d_0(\tilde{a})^3+\frac{1}{24}\sum_{i=0}^{n-1}b_i(\eta_n-\eta_i)_+^4=\lambda_0,$$

$$a_1+a_2(\tilde{a})+\frac{1}{2}d_0(\tilde{a})^2+\frac{1}{6}\sum_{i=0}^{n-1}b_i(\eta_n-\eta_i)_+^3=\lambda_1,$$

$$a_1+a_2(\tilde{b})+\frac{1}{2}d_0(\tilde{b})^2+\frac{1}{6}\sum_{i=0}^{n-1}b_i(\eta_n-\eta_i)_+^3=\lambda_2.$$

The boundary conditions at zero are satisfied by the following initial curves $f(\eta)=0.25\eta^2+B\eta$ and $\theta(\eta)=-\eta+1$. Hence, the value of f_m,θ_m and their derivatives are obtained from the initial curves. To acquire the complete solution of Eq. (25) and Eq. (26), we need to solve Eq. (28) and Eq. (29) to gather with the boundary conditions using Eq. (13) and Eq. (14) in order to find the values of the following unknowns $a_0,a_1,a_2,b_0,b_1,b_2,...,b_{n-1},d_0,d_1,d_2,...,d_{n-1}$.
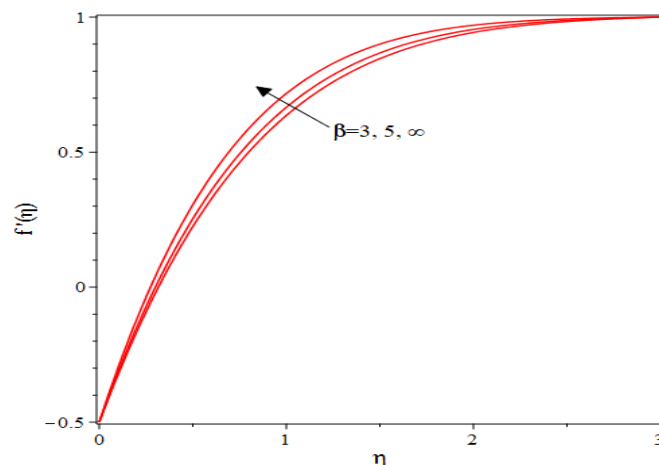
Fig. 6 The impact of Casson fluid parameter β on the velocity profile $f'(\eta)$.
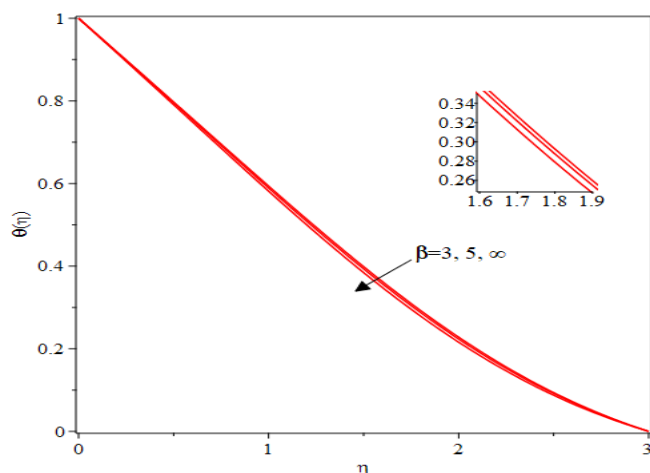
Fig. 7 The impact of Casson fluid parameter β on the temperature profile $\theta(\eta)$.

5. RESULTS AND DISCUSSION

The In this section, the obtained approximate solutions using collocation method based on spline functions for Eq. (13) and Eq. (14) are analyzed. The condition $f'(H) = 1$ is used instead of the condition $f'(\infty) = 1$ for some sufficiently large H. The obtained solutions of the proposed problem are investigated to illustrate the properties of Casson fluid flow in the presence of magnetic field. The non-dimensional parameters are considered as $M = 1, B = -0.5, \beta = \infty, \mathrm{Pr} = 0.7$, and $Nr = 3$ in the numerical results except the variations. In the illustrative graphs, the gold color profiles and red color profiles are represented the flow of non-Newtonian Casson fluid and the flow of Newtonian fluid, respectively. Fig. 2 and Fig. 3 illustrate the influence of the shrinking parameter B on the velocity profile and temperature profile, respectively, for both Casson and Newtonian fluids. The velocity profiles $f'(\eta)$ decreases with decreasing the magnitude of shrinking parameter B while the temperature profile increases with decreasing the value of shrinking parameter. Fig. 4 and Fig. 5 show the influence of M on the velocity profile and temperature profile, respectively. We detect that the velocity profile $f'(\eta)$ is enhanced with increasing values of the magnetic field parameter M whereas the temperature profiles and thermal boundary layer thickness decrease with increasing values of magnetic field parameter M. Fig. 6 depicts the effect of the dimensionless Casson fluid parameter β on the velocity profile for both Casson and Newtonian fluids. It is observed that a hike in the value of β enhances the velocity profiles whereas one can observe depreciation in the temperature profiles in Fig. 7 due to rising the values of β for both Casson and Newtonian fluids.

Fig. 8 and Fig. 9 elucidate the strength of the Prandtl number Pr and thermal radiation parameter Nr on the temperature profiles, respectively. It reveals that the thermal boundary layer thickness is depreciate with increasing the values of the Prandtl number Pr and the radiation parameter Nr. From Fig. 8 and Fig. 9 one can observe that with the reduction of the Prandtl number Pr and the radiation parameter Nr the thermal boundary layer thickness experiences an increasing trend. Hence, for bigger Prandtl number the liquid has a low temperature conductivity, that decline the correspondent thermal boundary layer thickness. Thus, the heat transfer rate is increased at the surface with improving Prandtl number Pr. In addition, for higher radiation parameter Nr the thinning of the thermal boundary thickness is occurred. Here, one

can utilize the radiative mode of heat transfer to increase the sheet heat loss. Finally, Fig. 10 and Fig. 11 illustrate the influence of α on the velocity profile and temperature profile, respectively. From Fig. 10 and Fig. 11 we conclude that depreciation in the values of α cause reduction in the velocity profile and thermal boundary thickness.

Table 1 The effect of shrinking parameter B on $f''(0)$ and $-\theta'(0)$.

M	CMSF $f''(0)$	CMSF $-\theta'(0)$	FDD $f''(0)$	FDD $-\theta'(0)$	RK4 $f''(0)$	RK4 $-\theta'(0)$
0.0	1.495673	0.346041	1.495722	0.346172	1.49567	0.34603
0.5	1.674182	0.356415	1.674222	0.356736	1.67418	0.35641
1.0	2.120147	0.378352	2.120137	0.379832	2.12019	0.37834
1.5	2.703645	0.400742	2.703497	0.405899	2.70376	0.40073

The comparison of values of skin friction and heat transfer rate at the sheet for shrinking parameter B with the presence of magnetic field is given in Table 1. The wall shear stress $f''(0)$ enhances for $0.25 \leq -B \leq 1.25$ whereas a reverse trend can be observed for $1.25 \leq -B \leq 2.0$. The influence of applied magnetic field on the wall shear stress $f''(0)$ and heat transfer rate $-\theta'(0)$ is illustrated in Table 2. It can be seen from Table 2. that the values of shear stresses $f''(0)$ increases due to increment in the values of magnetic parameter while the heat transfer rate from the sheet experience depreciation with increment in the values of M. Hence, the impinging flow is assisted by the transverse magnetic field and decreases the horizontal and vertical flow reversal as depicted in Fig. 4. Finally, in Table 3. the comparison of values of shear stress $f''(0)$ is described. We found from tables that the present results using are in an excellent agreement with that of (Lok et al., 2006; Wang 2008; Ashraf and Rashid, 2012), and Runge Kutta method.

Table 2 The effect of magnetic field parameter M on $f''(0)$ and $-\theta'(0)$.

$-B$	CMSF $f''(0)$	CMSF $-\theta'(0)$	FDD $f''(0)$	FDD $-\theta'(0)$	RK4 $f''(0)$	RK4 $-\theta'(0)$
0.25	1.877458	0.411450	1.877455	0.412803	1.877460	0.41144
0.50	2.120148	0.377394	2.120114	0.378822	2.120190	0.37739
1.00	2.429951	0.300877	2.429972	0.302334	2.429962	0.30086
1.25	2.476297	0.256815	2.476343	0.258227	2.476281	0.25680
1.50	2.425857	0.207058	2.425917	0.208447	2.425803	0.20704
2.00	1.805775	0.076266	1.805761	0.076282	1.805569	0.07624

following are the common errors in formatting the paper and should be avoided:

6. CONCLUSIONS

This paper considers the two-dimensional MHD stagnation point Casson fluid flow over a continuous moving sheet and heat transfer of an electrically conducting fluid towards a heated shrinking surface. The quasi-linearization technique is used to convert the non-linear equations of the model to a system of linear equations and then solved by the collocation method based on the spline function. The comparison of the present results with the numerical results previously reported and the effect of the emerged physical parameters on the velocity profiles and temperature profiles are shown through tables and illustrative graphs. This work has shown that:
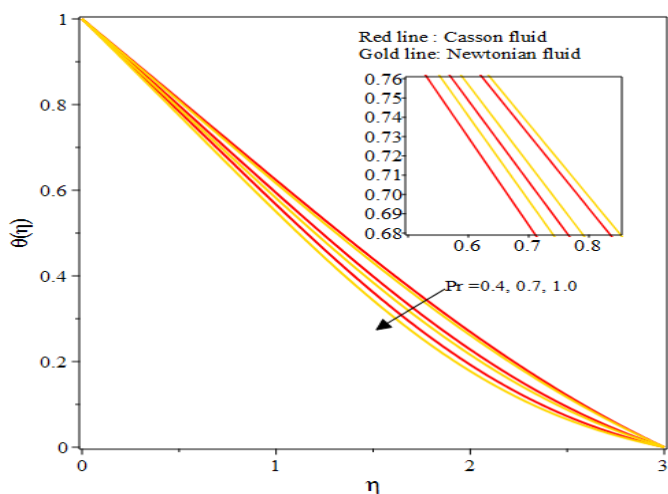
Fig. 8 The impact of Prandtl number Pr on the temperature profile.
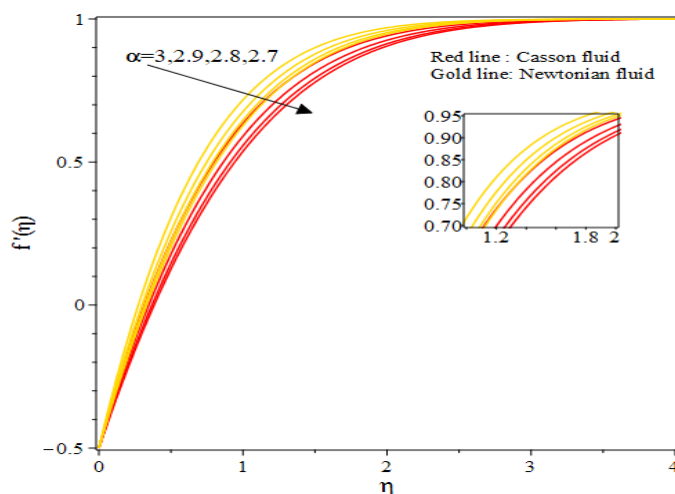
Fig. 10 The impact of α on the velocity profile $f'(\eta)$.
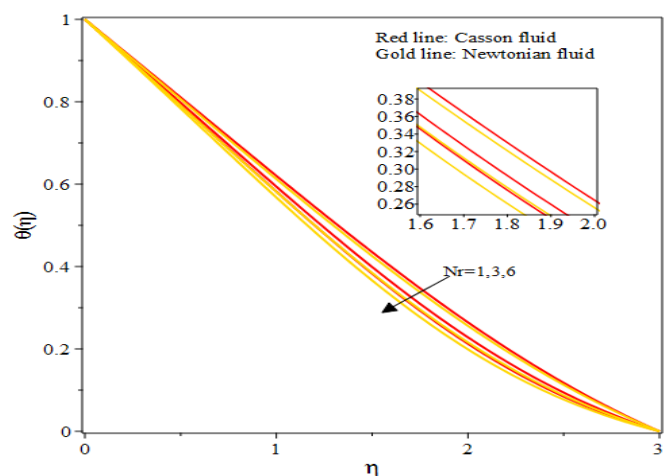
Fig. 9 The impact of radiation parameter Nr on the temperature profile.

Fig. 11 The impact of α on the temperature profile $\theta(\eta)$.

Table 3 Comparison of values of skin-friction $f''(0)$ for two values of B.

B	CMSF	FDD	RK4	Wang(2008)	Lok et al.(2006)
0.2	1.05113	1.05112	1.05113	1.05113	1.05129
0.5	0.71330	0.71328	0.71329	0.71330	0.71334
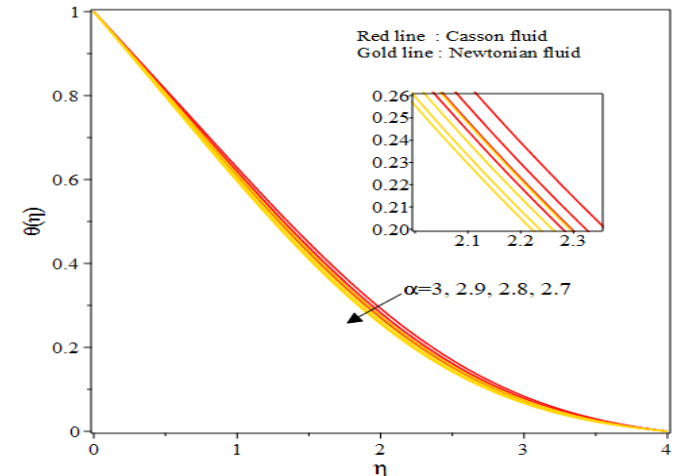
i.   The temperature profiles depreciate with improvement in the values of Prandtl number and thermal radiation for Casson and Newtonian fluids.

ii. An increment in the value of dimensionless Casson fluid parameter, shrinking parameter, and magnetic field parameter decline the thermal distribution while it experiences an improvement with increasing the value of α for both Casson and Newtonian fluids.

iii. The skin friction $f''(0)$ improves for $0.25 \le -B \le 1.25$ while a reverse trend is observed for $1.25 \le -B \le 2.0$. However, the heat transfer rate $-\theta'(0)$ increases with depreciation in the value of the shrinking parameter.

iv. The magnetic field considerably effects the skin friction and the heat transfer rate. The skin friction enhances due to increment in the magnetic field parameter for Casson and Newtonian fluids while the rate of the heat transfer depreciates when the value of magnetic parameter improves.

v.   Finally, we conclude that the suggested method is a good tool and an efficient technique to solve boundary layer problems.

NOMENCLATURE

a,b	real values
B	shrinking parameter
x	horizontal coordinate
y	vertical coordinate
U	free stream
f	dimensionless stream function
u,v	velocity components
Pr	Prandtl number
Nr	radiation parameter
t	time
T	temperature of the fluid
q	radiative heat flux
M	magnetic parameter

| k | Stefan-Boltzmann constant |

Greek Symbols

α	fractional order derivative
η	similarity variable
β	Casson fluid parameter
κ_0	heat conductivity
θ	dimensionless temperature
σ	absorption coefficient

REFERENCES

Al-Sawalmeh, M. 2022, "Numerical analysis of Casson ferro-hybrid nanofluid flow over a stretching sheet under constant wall temperature boundary condition," *Frontiers in Heat and Mass Transfer (FHMT)*, 18. https://doi.org/10.5098/hmt.18.12

Ashraf, M., and Rashid, M. 2012, "MHD Boundary Layer Stagnation Point Flow and Heat Transfer of a Micropolar Fluid towards a Heated Shrinking Sheet with Radiation and Heat Generation," *World Appl. Sci. J,* 16 (10), 1338–51.

Babu, M. , Gangadhar, K. and M Lavanya. 2017. "MHD Boundary Layer Flow of Casson Nanofluid over a Vertical Exponentially Stretching Cylinder under Newtonian Heating," *Research Journal of Pharmacy and Technology*, 10 (4), 998–1010. https://doi.org/10.5958/0974-360X.2017.00181.0

Baby, R., Kumar, C. H., and Rao, A. V. 2021, "MHD Casson Fluid Flow along Inclined Plate with Hall and Aligned Magnetic Effects," *Frontiers in Heat and Mass Transfer (FHMT),* 17. https://doi.org/10.5098/hmt.17.2

Bickley, W. G. 1968, "Piecewise Cubic Interpolation and Two-Point Boundary Problems," *The Computer Journal*, 11 (2), 206–8.https://doi.org/10.1093/comjnl/11.2.206

Boor, Carl De, and Carl De Boor. 1978, *A Practical Guide to Splines*. 27. springer-verlag New York.

Casson, N. 1959, "A Flow Equation for Pigment-Oil Suspensions of the Printing Ink Type," *Rheology of Disperse Systems*.

Crane, L. J. 1970, "Flow Past a Stretching Plate," *Zeitschrift Für Angewandte Mathematik Und Physik ZAMP*, 21 (4), 645–47. https://doi.org/10.1007/BF01587695

Dhange, M, Sankad, G., and Maharudrappa, I. 2022, "Casson fluid flow due to stretching sheet with magnetic effect and variable thermal conductivity," *Frontiers in Heat and Mass Transfer (FHMT),* 18. https://doi.org/10.5098/hmt.18.36

El-Aziz, A., and Afify, A. 2019, "MHD Casson Fluid Flow over a Stretching Sheet with Entropy Generation Analysis and Hall Influence," *Entropy,* 21 (6), 592. https://doi.org/10.3390/e21060592

El-Aziz, A., and Afify, A. 2016, "Effects of Variable Thermal Conductivity with Thermal Radiation on MHD Flow and Heat Transfer of Casson Liquid Film over an Unsteady Stretching Surface," *Brazilian Journal of Physics* 46 (5), 516–25.

https://doi.org/10.1007/s13538-016-0442-3

Ganesh, G., and Sridhar, W. 2021, "Numerical Approach of Heat and Mass Transfer of MHD Casson Fluid under Radiation over an Exponentially Permeable Stretching Sheet with Chemical Reaction and Hall Effect," *Frontiers in Heat and Mass Transfer (FHMT)* 16. https://doi.org/10.5098/hmt.16.5

Goswami, S., and Sarma, D. 2021, " The simultaneos effect of eckert number and magnetic prandtl number on Casson fluid flow," *Frontiers in Heat and Mass Transfer (FHMT),* 16. https://doi.org/10.5098/hmt.16.12

Gupta, P. S., and Gupta, A. S. 1977, "Heat and Mass Transfer on a Stretching Sheet with Suction or Blowing," *The Canadian Journal of Chemical Engineering*, 55 (6), 744–46. https://doi.org/10.1002/cjce.5450550619

Hayat, T, Saleem, N., and Ali, N . 2010, "Effect of Induced Magnetic Field on Peristaltic Transport of a Carreau Fluid," *Communications in Nonlinear Science and Numerical Simulation*, 15 (9), 2407–23. https://doi.org/10.1016/j.cnsns.2009.09.032

Hiemenz, K. 1911. "Die Grenzschicht an Einem in Den Gleichformigen Flussigkeitsstrom Eingetauchten Geraden Kreiszylinder," *Dinglers Polytech J.,* 326, 321–24.

Izyan, M. D. Nurul, Viswanathan, K. K., Aziz, Z. A., Lee, J. H., and Prabakar, K . 2017, "Free Vibration of Layered Truncated Conical Shells Filled with Quiescent Fluid Using Spline Method," *Composite Structures,* 163, 385–98. https://doi.org/10.1016/j.compstruct.2016.12.011

Khan, M., Elkotb, R. M., Matoog, R. T., Alshehri, N. A., and Abdelmohimen, M. A. H. 2021, "Thermal Features and Heat Transfer Enhancement of a Casson Fluid across a Porous Stretching/Shrinking Sheet: Analysis of Dual Solutions," *Case Studies in Thermal Engineering*, 28, 101594. https://doi.org/10.1016/j.csite.2021.101594

Lok, Y. Y., Amin, N., and Pop, I. 2006, "Non-Orthogonal Stagnation Point Flow towards a Stretching Sheet," *International Journal of Non-Linear Mechanics*, 41 (4), 622–27. https://doi.org/10.1016/j.ijnonlinmec.2006.03.002

Mahanta, G., and Shaw, S. 2015, "3D Casson Fluid Flow Past a Porous Linearly Stretching Sheet with Convective Boundary Condition," *Alexandria Engineering Journal*, 54 (3), 653–59. https://doi.org/10.1016/j.aej.2015.04.014

Malik, M. Y., Naseer, M., Nadeem, S., and Abdul Rehman. 2014, "The Boundary Layer Flow of Casson Nanofluid over a Vertical Exponentially Stretching Cylinder," *Applied Nanoscience*, 4 (7), 869–73. https://doi.org/10.1007/s13204-013-0267-0

Malo, D. H., Murad, M. A. S., Masiha, R. Y., and Abdulazeez, S.T. 2021, "A New Computational Method Based on Integral Transform for Solving Linear and Nonlinear Fractional Systems," *Jurnal Matematika MANTIK*, 7 (1), 9–19. https://doi.org/10.15642/mantik.2021.7.1.9-19

Mandelzweig, V. B., and Tabakin, F. 2001, "Quasilinearization Approach to Nonlinear Problems in Physics with Application to Nonlinear ODEs," *Computer Physics Communications*, 141 (2), 268–81.

https://doi.org/10.1016/S0010-4655(01)00415-5

Mekheimer, K. S. 2008, "Effect of the Induced Magnetic Field on Peristaltic Flow of a Couple Stress Fluid," *Physics Letters A*, 372 (23), 4271–78.
https://doi.org/10.1016/j.physleta.2008.03.059

Murad, M. A. S. 2022. "Modified Integral Equation Combined with the Decomposition Method for Time Fractional Differential Equations with Variable Coefficients," *Applied Mathematics-A Journal of Chinese Universities* 37 (3), 404–14.
https://doi.org/10.1007/s11766-022-4159-5

Murad, M. A. S., and Hamasalh, F. K. 2022, "Computational Technique for the Modeling on MHD Boundary Layer Flow Unsteady Stretching Sheet by B-Spline Function," In *2022 International Conference on Computer Science and Software Engineering (CSASE)*,236–40, IEEE.
https://doi.org/10.1109/CSASE51777.2022.9759738

Parand, K., Shahini, M., and Dehghan, M. 2009. "Rational Legendre Pseudospectral Approach for Solving Nonlinear Differential Equations of Lane–Emden Type," *Journal of Computational Physics*, 228 (23), 8830–40.
https://doi.org/10.1016/j.jcp.2009.08.029

Raju, C. S. K., and Sandeep, N. 2016. "Unsteady Three-Dimensional Flow of Casson–Carreau Fluids Past a Stretching Surface," *Alexandria Engineering Journal*, 55 (2), 1115–26.
https://doi.org/10.1016/j.aej.2016.03.023

Raju, R., Reddy, G., and Anitha, G. 2017, "MHD Casson Viscous Dissipative Fluid Flow Past a Vertically Inclined Plate in Presence of Heat and Mass Transfer: A Finite Element Technique," *Frontiers in Heat and Mass Transfer (FHMT)*, 8.
https://doi.org/10.5098/hmt.8.27

Raptis, A., Perdikis, C., and Takhar, H. S. 2004, "Effect of Thermal Radiation on MHD Flow." *Applied Mathematics and Computation*, 153 (3), 645–49.
https://doi.org/10.1016/S0096-3003(03)00657-X

Sakiadis, B. C. 1961. "Boundary-layer Behavior on Continuous Solid Surfaces: II. The Boundary Layer on a Continuous Flat Surface," *AiChE Journal*, 7 (2), 221–25.
https://doi.org/10.1002/aic.690070211

Sandeep, N., Sugunamma, V., and Mohankrishna, P. 2013, "Effects of Radiation on an Unsteady Natural Convective Flow of a EG-Nimonic 80a Nanofluid Past an Infinite Vertical Plate," *Advances in Physics Theories and Applications*, 23, 36–43.

Schumaker, L. L. 2015, *Spline Functions: Computational Methods*, SIAM.
https://doi.org/10.1137/1.9781611973907

Shehzad, S. A., Hayat, T., and Alsaedi, A. 2015, "Three-Dimensional MHD Flow of Casson Fluid in Porous Medium with Heat Generation," *Journal of Applied Fluid Mechanics*, 9 (1), 215–23.
https://doi.org/10.18869/acadpub.jafm.68.224.24042

Shercliff, J, A. 1965, "A Textbook of Magnetohydrodynamics," Pergamon, Oxford.

Wang, C. Y. 2008, "Stagnation Flow towards a Shrinking Sheet," *International Journal of Non-Linear Mechanics*, 43 (5), 377–82.
https://doi.org/10.1016/j.ijnonlinmec.2007.12.021.